

RESEARCH ARTICLE

Identify Direct Lightning Strike Location Based on Discrete Wavelet Transform for 115-kV Transmission System

PATHOMTHAT CHIRADEJA¹ AND ATTHAPOL NGAOPITAKKUL^{1,2}¹Faculty of Engineering, Srinakharinwirot University, Bangkok 10110, Thailand²School of Engineering, King Mongkut's Institute of Technology Ladkrabang, Bangkok 10520, Thailand

Corresponding author: Atthapol Ngaopitakkul (atthapol.ng@kmitl.ac.th)

ABSTRACT This paper proposes three techniques for locating lightning strikes in a 115 kV transmission system over 88.5 km, based on the arrival time of a transient wave obtained from a discrete wavelet transform (DWT). The first technique calculates the location based on the 'type D' travelling wave method. The second technique analyses the first arrival time and same reflected-back wave arrival time between two substations. In the third technique, two sensors are installed to record arrival times at each sensor. Case studies of direct lightning strikes to phase conductors (shielding failure) are simulated using the 'Alternative Transients Program/Electromagnetic Transients Program' (ATP/EMTP). The influences of three parameters are considered: inception angles, the phase of the conductor, and the position at which the lightning struck the transmission system. By performing an operation scheme for all techniques, a positive sequence current is calculated, using a three-phase current from the ATP/EMTP program which is converted using Clark's transform. A positive sequence current is extracted to several scales using the DWT, and the orders of arrival times for both substations are determined. After the arrival times are obtained, each technique uses a different order of arrival time for calculating the lightning location. By comparing the average error among the three techniques, it is shown that the arrival time of the two sensors' technique is less than that of the other techniques.

INDEX TERMS Discrete wavelet transforms, lightning protection, lightning location, power system transients, transmission lines, travelling wave.

I. INTRODUCTION

The demand for electricity has continuously risen with the expansion of urban areas and population. In addition, economic growth also contributes to increasing electrical consumption. This is particularly evident in the business and industrial sectors of Thailand, which is transitioning from an agricultural to an industrial society. This trend directly influences the government's decisions to expand the capacity of the generation, transmission, and distribution networks, so as to support future growth. However, the expansion of the power system may increase the rate of lightning strikes in a transmission system, even when the overhead ground wire is

protected. A lightning strike is a natural phenomenon caused by an electric discharge from the atmosphere to an object on the ground. A direct strike on a transmission line can cause a massive impact on the overall power system [1]; it can generate heat [2], an electromagnetic field [3], a high electric current amplitude [4], or a transient signal, and an overvoltage [5] from the discharge can cause power outage, thereby influencing the reliability and stability of the power system. There is a high probability of lightning striking the overhead ground wire, the ground near the transmission tower, and the conductor, owing to the nature of lightning phenomena. Lightning often strikes the overhead ground wire but causes insignificant damage to the power system, whereas lightning rarely strikes the conductor, but causes serious damage to the power system [4]. Thus, ensuring the reliability of the power

The associate editor coordinating the review of this manuscript and approving it for publication was Fabio Mottola¹.

system requires a well-designed protection system, accuracy in identifying the strike location, and the speed to restore the system following a problem.

Several technologies and networks of communication such as lightning location system (LLS), lightning mapping array (LMA) were used to create a lightning map by required components of transmission network. [6]–[9]. The presented technologies can be classified the type of lightning and analyzed the characteristics of a lightning strike [7], [8].

According to the study focused on a characteristic [10]–[22], lightning signals included return strikes, channel of current [10], upward lightning, potential lightning [11], [12], velocity and etc. were considered. Moreover, the result in research [15]–[22] found that environment around the transmission tower [16], transmission line modelling (TLM) methodology [17] and grounding of transmission tower [18], [19] influence the lightning strike and thus the current, voltage, and waveform of a transient signal travelling through a conductor [21], [22]. Thus, these was the key components of an algorithm which can accurately locate lightning strikes during transmission.

Three typical techniques used by the lightning location systems cost of time of arrival [23], magnetic direction finding [24] and interferometry [25], which been used to applied on broader lightning location. For the direct lightning strike on conductor, many techniques are used to identify abnormal positions, and they are not only used for locating lightning, but are also able to compute fault locations. These techniques include phasor measurement [26]–[32], travelling waves [33]–[39], a discrete wavelet transform [40]–[47], and artificial intelligence [48]–[51], among others.

First, the phasor measurement method (PMU) commonly requires parameters of voltage [26], current, and impedance to identify the lightning location [27]. However, even the PMU has acceptable performance for lightning signal analysis [28], but the one imperfection of this method was the result was proved in simple power system. Observing complex system requires a larger amount of data, and many measurement units. This cause long processing time and the calculating data might loss. It resulted in the accuracy and reliability decrease.

The travelling wave technique is based on the natural aspects of an electromagnetic wave which results from the disturbance in a conductor during the transient state. Its properties can be widely applied to locate a disturbance in a power system [33]–[39]. The research proposed a novel algorithm to detect and identify the stepped leader stage and lightning channel height of cloud-to-ground lightning using the electric field [33]. Traveling-waved-based fault-location methods have the advantage of less interference from the saturation characteristics of the current transform, as well as the fault resistance, fault type, and operating mode of system; thus, these methods have been successfully applied to locating faults in transmission networks. A developed a method based on using synchronized travelling waves to identify lightning strike locations on transmission lines or

the ground has been proposed [35]. Protection relays based on an ellipsoidal pattern were used for signal processing and transient signal detection. The author claims that the proposed method is simpler and more accurate than using a distance protection relay with a wavelet.

The velocity of the transient wave and the time difference between the first arrival time and the same reflected wave are analysed [36]–[39]. Thus, conventional fault location methods can be divided into impedance-focused methods (phasor or time-domain based) and travelling wave-based methods. The effectiveness of the travelling wave technique in fault location depends on the accuracy of the obtained signal. However, processing for obtaining the signal, such as the discrete wavelet transform (DWT), must be implemented to correctly calculate and locate the disturbance.

The DWT is a mathematic methodology for signal processing, and is a similar concept to its predecessors like the Fourier transform. However, the difference is in the ability to process signals in the frequency domain, instead of the time domain. It has recently gained greater attention in the field of power systems, owing to a wide range of applications in disturbance analysis on various power system components [40]–[44] such as generators [40], motors [41], and transformers [42]. It can be seen that the DWT has a wide range of application in disturbance analysis in various situations such as faults, lightning, and transient switching [43]–[46].

A lightning locating methodology might have a significant error, which can affect the performance of a protection system [47]. Thus, better lightning-locating algorithms with increased accuracy need to be developed to ensure the reliability of systems. In addition, various parameters such as the peak value of lightning, structure of the transmission system, and material of the equipment can affect the velocity of travelling waves. These can cause errors in the process of calculating the location. A combination of the DWT and the travelling wave method is a commonly-used method for locating a disturbance in a transmission system, owing to the ability to adjust frequency limitation and to extract the arrival time of a transient wave when a lightning strike occurs.

Artificial intelligence is also a new research field, insofar as its application in locating disturbances in power system [48]–[51]. The artificial neural network is a high-efficiency methodology with satisfying accuracy in locating disturbances on a transmission network, but it has limitations in complex decision conditions, and requires a significant amount of input from instruments to accurately locate a fault. An acoustic technique using a noise signal in a transmission line and neural network to classify the obtained signal has been used to detect faults in insulators [51]. From the literature review, it is evident that disturbance-locating algorithms have applied methodologies such as travelling waves, electromagnetic fields, artificial neural networks, and the DWT. These techniques have different advantages and usage restrictions generated from the frequency, noise limitations, data requirements, and training time. However, the

discussion regarding these methodologies mainly focuses on fault location, and rarely focuses on locating lightning strikes on a transmission line, even though the effect of a lightning strike can be severe to devices and equipment in transmission system, which directly affects the reliability of the system and has wide-ranging impact on end-users.

This paper aims to propose three methodologies for locating a lightning strike in a 115 kV transmission system, based on a combination of the travelling wave method and the DWT. A lightning strike signal and transmission system are simulated using ATP/EMTP and MATLAB software. An instrument installed on a substation is used for retrieving voltage and current signals under both normal and lightning conditions. The obtained data are analysed by using the DWT to extract a high-frequency component on different wavelet scales along with its coefficient value, which is then used with travelling waves to calculate the location of a lightning strike. The originality and main contributions of this paper are as follows:

- Three techniques based on the DWT to identify the location of a lightning strike in a transmission system are presented and compared.
- The system under study is modelled on a part of a 115-kV transmission line in the 'Electricity Generating Authority of Thailand' (EGAT) network, and various parameters which can affect the performance of the methodologies, such as inception angle, inception phase, and location of the lightning strike, are taken into consideration.
- The performance of the proposed methodology is evaluated by testing it on the transmission system under different conditions, and verifying the accuracy of the lightning location(s).

The remainder of this paper is organized as follows. Section II presents travelling wave and proposed technique used to locate the lightning strike in the transmission system. In Section III, simulation is implemented. Section IV discusses simulation results. Finally, Section V offers conclusions, summarizes the main contributions, and suggests directions for future work.

II. TRAVELLING WAVE AND PROPOSED TECHNIQUE

There is no perfect electrical system on earth; thus, electrical systems must compensate when a fault occurs in the transmission system. In most power system-relaying algorithms, the first step always involves fault detection, and the next step involves fault identification, as well as fault location. The information related to detection of faults is essential for the fault location algorithm. As previously mentioned, the most effective technique for calculating fault location has been proposed based on a travelling wave.

Overhead line Fault location based on travelling waves can be divided into five types: A, B, C, D, and E, based on the measuring method used. However, in modern fault location, type A (sometimes called a single-end method) and

type D (sometimes called a double-end method) are the most commonly used methods. Type A only requires considering two time situations, that is, a transient wave travelling from one observed substation, and the same wave being reflected back. Type D requires the time which wave takes to travel from the sending and receiving substations, and disregards the reflected wave.

As depicted in Fig. 1, when a fault occurs in a transmission line, a transient wave appears at the position of the fault, and the transient wave travels to the end of the line with velocity close to speed of light. The first arrival time of the transient wave travelling from the position of the fault to the end of the sending substation is recorded by the current transformer (CT), and is defined as t_{1stRYG} . Subsequent to first arrival time, the transient wave is reflected back to the position of the fault, and then back again to the end of the sending substation. The arrival time of the reflected wave is also recorded by the CT at the sending substation, and is defined as t_{3rdRYG} , or the third-order arrival time of the transient wave which arrives at the sending substation. As previously mentioned, t_{1stRYG} and t_{3rdRYG} are considered as input data for calculating a fault location based on the type A travelling wave method. Similarly, by considering the receiving substation as shown in Fig. 1, it can be observed that the transient wave behaviour in travelling to the end of the receiving substation is the same as that to the sending substation, such that t_{1stCTI} and t_{3rdCTI} are the first arrival time and the time of reflected-back wave corresponding to the first arrival time, respectively. Hence, t_{1stRYG} and t_{1stCTI} are considered as input data for calculating a fault location based on the type D travelling wave method. Moreover, by considering the sending substation in Fig. 1, the first arrival time of the transient wave at the receiving substation (t_{1stCTI}) will be reflected back through the position of the fault to the other end of the line. The transient wave which travels past the position of the fault to the opposite end is denoted as t_{2ndRYG} . However, in case of a fault location occurring near the sending substation, the order of arrival times of t_{3rdRYG} and t_{2ndRYG} would change; this indicates that the order of arrival times of transient waves is necessary for studying travelling waves. In this regard, the arrival time of the transient wave travelling to the end of line depends on the length of the transmission line and the position of the fault. This indicates that the calculation of fault location can benefit from the variations of the arrival time.

Similarly, when a lightning strike occurs, the lightning position generates a lightning pulse. The pulse, which has high energy owing to the energy of lightning, transfers to the lightning point and travels to the end of the line. It is necessary to accurately determine the lightning location to reduce the time of failure interruption, quickly restore the power supply, and improve reliability. To realise this, a high-accuracy lightning location technique is essential. This study investigated three techniques for identifying a lightning location based on travelling waves and the DWT. All techniques were based on travelling waves, as the travelling wave technique was one technique which was able to locate lightning strike in the

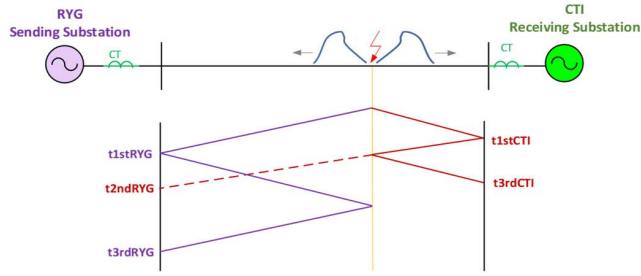


FIGURE 1. Bewley lattice diagram for transient wave in transmission line.

transmission system. Moreover, all proposed techniques used the arrival time to calculate the lightning location. The first technique calculated the location by using a travelling wave (based on the type D travelling wave method). The second technique calculated the location by using time of arrival of the transient wave (based on the type A and D travelling wave methods), and the third technique calculated the location by using the distribution section of the transmission line. Thus, all techniques used the arrival time, but the order of arrival time was different, as follows.

Method 1: Calculate location by using travelling wave (based on the type D travelling wave method) [52], [53].

A method for determining a lightning strike location based on the combination of the travelling wave type D and a wavelet transform was proposed, as shown in Equation 1. The technique reflected in Equation 1 is based on two main parameters; the first arrival time of the transient wave, and the velocity wave which travels to the end of both substations. Generally, GPS receivers are installed at transmission line ends in a substation. Synchronization between the arrival times of the transient wave is realised by using a GPS receiver to obtain the time differences in when transient waves reach substation. As shown in Fig. 1, when the sending-end (RYG) substation is considered during a lightning strike, t_{1stRYG} is the first arrival time which can be used to detect abnormal conditions at sending end, whereas when the receiving end is also considered during the lightning strike, t_{1stCTI} is the first arrival time which can be used to detect abnormal conditions at the receiving end. Hence, t_{1stRYG} and t_{1stCTI} are considered as input data for Equation 1.

When the velocity of a travelling wave is carefully considered as shown in Fig. 2 and the data in Table 1, a relation between the velocity of the travelling wave and the frequency band can be found. This indicates that the velocity of a travelling wave depends on frequency band, as shown in Table 1. This research observed lightning events in which frequency of the lightning was higher than normal conditions; in that regard, the sampling frequency rate used for the simulation was 200 MHz (corresponding to the chosen sampling time used in ATP/EMTP, which is 5 ns). Thus, the velocity of the travelling wave for calculating lightning location was 50–100 MHz at scale 1.

$$D = \frac{L - v(t_{1stCTI} - t_{1stRYG})}{2} \quad (1)$$

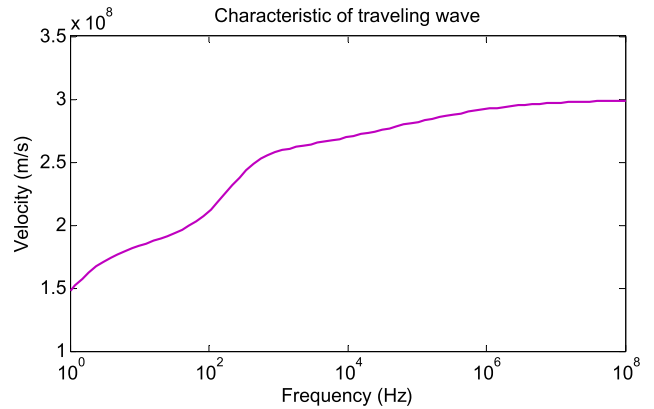


FIGURE 2. Relationship between velocity and frequency of travelling wave.

TABLE 1. Relationship between velocity and frequency band at each scale of wavelet transform.

Scale of Wavelet	Frequency range (MHz)	Average velocity (km/s)
1	50–100	298,782
2	25–50	298,354
3	12.5–25	297,749

In Equation 1:

- D = Measuring location referred from sending substation or RYG (km)
- L = Total distance of transmission line (km)
- t_{1stRYG} = first arrival time of transient wave travelling to sending substation (s)
- t_{1stCTI} = first arrival time of transient wave travelling to receiving substation (s)
- v = velocity of transient wave travelling in line (km/s)

Method 2: Calculate location by using time of arrival of transient wave (based on the type A and D travelling wave methods) [52], [54].

This technique is based on a combination of the travelling wave methods (type A and type D) and a wavelet transform, and has been proposed for improved fault location during simultaneous faults in an underground system [52], [54]. The obtained results show that, in the case of a simultaneous fault, this technique provides satisfactory results in locating faults. Equation 2 reflects the concept used in identifying the lightning location. The first arrival time and the same wave reflected back (or third order arrival time of transient wave) are used in this technique; this corresponds to the behaviour of the transient wave, as shown in Fig. 1. In view of Fig. 1, when the sending end is considered during a lightning strike, t_{1stRYG} and t_{3rdRYG} are the first arrival time and the arrival time of the same wave reflected back, respectively, and can be used to detect abnormal conditions at the sending end. In contrast, when the receiving end is considered during a lightning strike, t_{1stCTI} and t_{3rdCTI} are the first arrival time

and the arrival time of the reflected wave, and can be used to detect abnormal conditions at the receiving end. Hence, t_{1stRYG} , t_{3rdRYG} , t_{1stCTI} , and t_{3rdCTI} are considered as the input data for Equation 3, and 4. Moreover, this proposed method does not use the velocity of transient wave to calculate the lightning location.

$$D = \frac{L \times \Delta T_{RYG}}{\Delta T_{RYG} + \Delta T_{CTI}} \quad (2)$$

$$\Delta T_{RYG} = \frac{|T_{3rdRYG} - T_{1stRYG}|}{2} \quad (3)$$

$$\Delta T_{CTI} = \frac{|T_{3rdCTI} - T_{1stCTI}|}{2} \quad (4)$$

In the above:

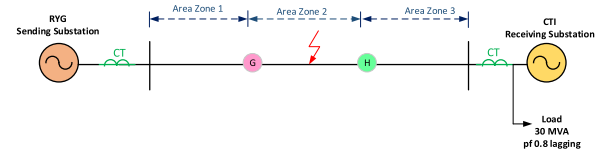
- D = measuring location reference at sending sub-station or RYG (km)
- L = total distance of transmission line (km)
- ΔT_{RYG} = differential arrival time between reflected wave and first wave which travelled to sending substation (s)
- ΔT_{CTI} = differential arrival time between reflected wave and first wave which travelled to receiving substation (s)
- t_{1stRYG} = first arrival time of transient wave which travelled to sending substation (s)
- t_{3rdRYG} = reflected back arrival time of transient wave which travelled to sending substation (s)
- t_{1stCTI} = first arrival time of transient wave which travelled to receiving substation (s)
- t_{3rdCTI} = reflected back arrival time of transient wave which travelled to receiving substation (s)

Method 3: Calculate location using two sensors.

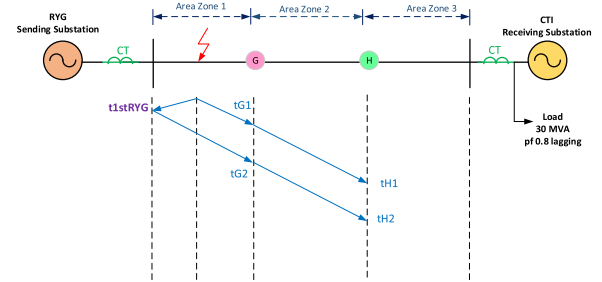
This technique is different from the above techniques, as the two previous techniques recorded the first arrival time and the arrival time of the same wave reflected back, whereas this technique involves installing two sensors in the transmission system. This not only records the time of first wave and the same wave reflected back, but also records the first and second arrival times where sensors G and H are installed. The two sensors are installed at $L/3$ and $2L/3$ of the transmission line to divide the length of the transmission line into three areas, as shown in Fig. 3(a). In Fig. 3(a), one substation (RYG) transfers power to another substation (CTI), and a transmission system links between the substations. Two sensors are installed on the conductor. During lightning strikes on the transmission line, the transient wave occurs at a position, and travels to each end of line.

For calculating the lightning location, the position of lightning depends on the area zones which the lightning strikes.

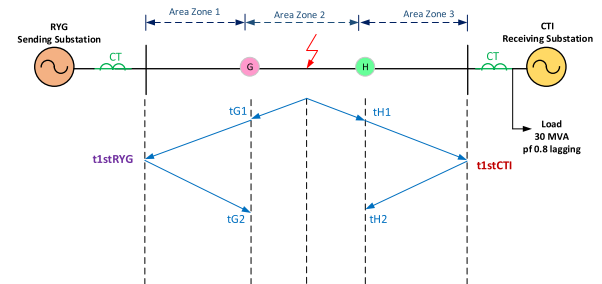
- Zone one: lightning strikes the line between sending substation (RYG) and sensor G.
- Zone two: lightning strikes the line between sensor G and sensor H.
- Zone three: lightning strikes the line between receiving substation (CTI) and sensor H.



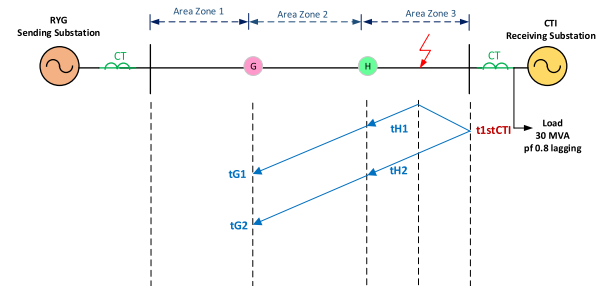
(a) Single-line diagram of two sensors installed in system.



(b) Behaviour of transient wave when lightning strikes in zone one.



(c) Behaviour of transient wave when lightning strikes in zone two.



(d) Behaviour of transient wave when lightning strikes in zone three.

FIGURE 3. Bewley lattice diagram for two sensors in transmission line.

In case of lightning strikes in zone one:

In Fig. 3(b), where lightning strikes between sending substation (RYG) and sensor G are considered, the lightning location is calculated using Equation 6. The sensors G and H are installed on the transmission line, and record the first and second arrival times to detect abnormal conditions. In this case, the first arrival time of sensor G will be recorded faster than the first arrival time of sensor H (at the receiving end), because the lightning occurs near the substation and sensor G. Hence, t_{G1} and t_{G2} are the first and second arrival times for detecting abnormal conditions at the sending end (RYG), whereas t_{H1} is the first arrival time for detecting abnormal

conditions at the receiving end (CTI).

$$v_1 = \frac{L}{3 |t_{G1} - t_{H1}|} \tag{5}$$

$$D = \frac{v_1 (t_{G2} - t_{G1})}{2} \tag{6}$$

- D = measuring location from sending substation or RYG (km)
- L = total distance of transmission line (km)
- v₁ = velocity of transient wave travelling within zone one (km/s)
- t_{G1} = first arrival time of transient wave at sensor G (s)
- t_{G2} = second arrival time (reflected back) of transient wave at sensor G (s)
- t_{H1} = first arrival time of transient wave at sensor H (s)

In case of lightning strikes in zone two:

In Fig. 3(c), where the lightning strikes between sensor G and sensor H, the lightning location is calculated using Equation 8. The sensors G and H are installed on the transmission line, and record the arrival times, which are t_{G1} and t_{H1}. Subsequently, the transient wave continues travelling to the end of the line. The CTs at both substations record t_{1stRYG} and t_{1stCTI}. The transient waves at both substations are reflected back, so the sensors G and H record the second arrival times as t_{G2} and t_{H2}.

$$v_2 = \left(\frac{\frac{L}{3}}{t_{G2} - t_{G1}} \right) + \left(\frac{\frac{L}{3}}{t_{H2} - t_{H1}} \right) \tag{7}$$

$$D = \frac{L + v_2 (t_{G1} - t_{H1})}{2} \tag{8}$$

- D = measuring location from sending substation or RYG (km)
- L = total distance of transmission line (km)
- v₂ = velocity of transient wave which travelling within zone two (km/s)
- t_{G1} = first arrival time of transient wave at sensor G (s)
- t_{G2} = second arrival time (reflected back) of transient wave at sensor G (s)
- t_{H1} = first arrival time of transient wave at sensor H (s)
- t_{H2} = second arrival time (reflected back) of transient wave at sensor H (s)

In case of lightning strikes in zone 3:

In Fig. 3(d), where the lightning strikes between sensor H and the receiving substation (CTI), it can be observed that the characteristic transient wave of zone three is similar to the characteristic transient wave of zone one, so that t_{H1} and t_{1CTI} are the arrival times of the detected transient wave at sensor H and the receiving end (CTI), respectively. The transient wave continues travelling to the sending substation.

Thus, sensor G can detect the arrival time, defined as t_{G1}. The lightning location is calculated using Equation 10. In that regard, t_{1stRYG} is reflected back to the direction of the sending substation. Thus, sensors H and G can record the second arrival time (reflected back), respectively.

$$v_3 = \frac{L}{3 |t_{H1} - t_{G1}|} \tag{9}$$

$$D = L - \frac{v_3 (t_{H2} - t_{H1})}{2} \tag{10}$$

- D = measuring location from sending substation or RYG (km)
- L = total distance of transmission line (km)
- v₃ = velocity of transient wave travelling within zone three (km/s)
- t_{G1} = first arrival time of transient wave at sensor G (s)
- t_{H1} = first arrival time of transient wave at sensor H (s)
- t_{H2} = second arrival time (reflected back) of transient wave at sensor H (s)

Owing to the use of this technique, the characteristics of the transient wave traveling on the transmission line depend on the area zone. If the characteristics are different, the equation used to calculate the lightning location is different. All behaviours are shown in Fig. 3(b) to Fig. 3(d).

The explanations in this section reflect the principles used in identifying lightning locations. Next, a simulation process using the ATP/EMTP program will be explained.

III. SIMULATION

The simulation of lightning event in this paper concern direct lightning strikes to phase conductors (shielding failure) of transmission line. Case studies of lightning locations were simulated using the ATP/EMTP program. The 115-kV system consists of sending substation (RYG) which transfers power to receiving substation (CTI) with a 150 MVA load. The distance between the two substations is 88.5 km, as shown in Fig. 4(a). A multi-story transmission tower model, that is, a transmission tower based on the transmission system of the EGAT, is shown in Fig. 4(b). In considering Fig. 4(b), the parameters of transmission tower model are based on the equations recommended by the Institute of Electrical and Electronics Engineers (IEEE) and the International Council on Large Electric Systems (CIGRE) [38]. The model is divided into four parts, and each part consists of a surge impedance (Z), resistance (R), and inductance (L), as shown in Fig. 4(b) and in the data in Table 2. In addition, the ground resistance of transmission tower (R_g) is determined as 10 ohm.

The circuit is simulated using the ATP/EMTP program, as shown in Fig. 4(c). In Fig. 4(c), in front of the substations, both substations have installed a current transformer, and between these two substations is a 7-transmission-towers model which is a double circuit/single conductor model

TABLE 2. Parameters of multi-story transmission tower.

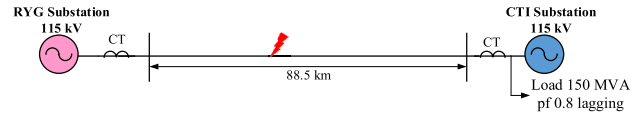
Parameters	$v = 300 \text{ m}/\mu\text{s}$				
	Z_1	R_1	L_1	Z_2	R_2
Z_1	180 Ω	12.39093 Ω	0.002495 mH	R_1	L_1
Z_2	180 Ω	13.89291 Ω	0.002797 mH	R_2	L_2
Z_3	180 Ω	13.89291 Ω	0.002797 mH	R_3	L_3
Z_4	140 Ω	31.24856 Ω	0.006291 mH	R_4	L_4

along the lines of American National Standards Institute (ANSI)/IEEE Std. C62.41. The peak value of the lightning, the line phase which lightning strikes, and the impulse of lightning are determined as unchanged, as shown in Table 3, whereas the inception angle, lightning position, and lightning phase are varied, as also shown in Table 3. Moreover, the surge source is a Heidler model which uses a lightning impulse with $3.1/77.5 \mu\text{s}$ [29]. The peak value of the lightning is 20 kA, and the lightning occurs at 0.002 s.

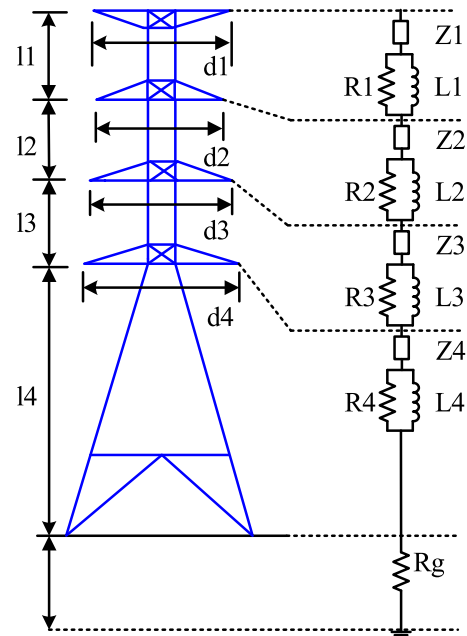
As shown in Table 3, the case study was simulated in the ATP/EMTP program with three variable parameters. First, the inception angle, which is the angle of voltage in reference with phase A, is varied from 0 to 150 degrees, and each step increased by 30 degrees. Second, the lightning position varied between 10% to 90% of the length as measured from the sending substation, with each step as 10%. Finally, the lightning phases were varied in the lightning simulation (i.e. phase A, phase B, and phase C).

The operation scheme has four steps, which are shown in Fig. 5. First, the current signal for each phase was simulated using the ATP/EMTP program. Next, using all of the current signals obtained from the simulation, a positive sequence current signal was calculated, and was converted with Clark’s transform using the all-phase current signal from the first step since in previous research [55] the all-phase current signal alone was insufficient for calculating lightning location. After the positive sequence was obtained, a DWT based on a ‘Daubechies 4 (db4)’ wavelet basis function was applied to the positive sequence current to decompose the high-frequency components of the signal into 3 levels. Finally, after applying the DWT, the arrival time of the transient wave was obtained from the DWT, so as to identify the lightning location with the proposed techniques. From the many case studies conducted, a case study of a lightning strike at 40% of the length of the transmission line is considered and is demonstrated as an example, as shown in Fig. 6.

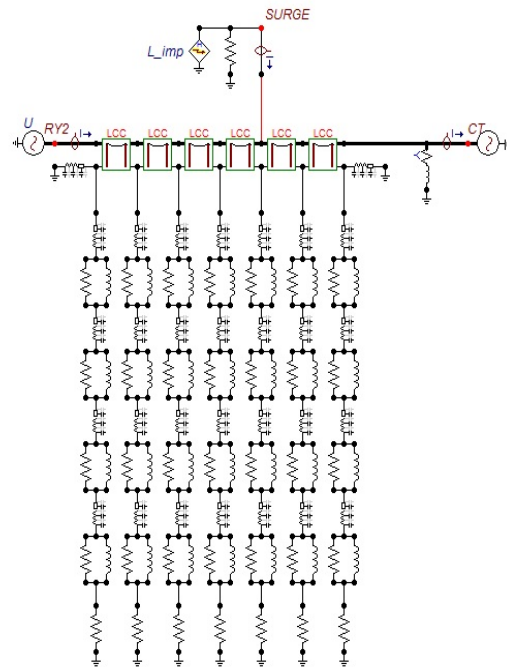
As noted above, an example of a lightning strike at 40% of the length of the transmission line is illustrated in Fig. 6. The three-phase current signals of the sending and receiving substations are plotted in Fig. 6(a) and Fig. 6(b), respectively. It can be observed that, after the lightning strike occurrence at 0.002 s, the obtained signal exhibits a sudden change in a short period of time (considering at 0.002 s) and is unsuitable for use in analysing lightning, as it has limited lag angles of phases A, B, and C. For the next step, the positive sequence current signal is converted with Clark’s transform with the all-phase current signal, as plotted in the top traces of Fig. 6(c) and Fig. 6(d). It can be observed that the peak



(a) Single-line diagram of the 115 kV transmission system.



(b) Multi-story transmission tower model used in the simulation.



(c) Components of the simulation circuit in Alternative Transients Program/Electromagnetic Transients Program (ATP/EMTP).

FIGURE 4. Transmission system for simulation.

value of positive sequence current tends to decrease with an increase in the period of time. Moreover, the first peak time of the positive sequence can be observed; this indicates that

TABLE 3. Simulation conditions.

Sending substation	RYG
Receiving substation	CTI
Load	150 MVA
Length of transmission line	88.50 km
Tower characteristic	
Tower Name	DA1
Conductor size	795 MCM ACSR/GA
Conductor characteristic	
Size	795 MCM ACSR/GA
Diameter	26.80 mm.
Number of conductors	1 conductor per bundle
Current capacity	845 A per conductor
Max. sag of conductor	10.55 m.
Overhead ground wire characteristic	
Size	3/8" (HS) Galvanised steel
Diameter	9.144 mm.
Number of conductors	1 conductor
System resistance	10 Ohm
Simulate condition	
Lightning time	0.002 seconds
Peak value of lightning current	20 kA by HEIDLER model
Inception angle	0–150 degrees (each step increases the angle by 30 degrees)
Position	10%–90% of the length (each step increases the distance by 10%)
Phase line	A B C

the first peak time can be beneficial in calculating lightning location. However, the first peak time of the transient wave cannot be clearly indicated, because this signal consists of different frequency ranges (high frequency and fundamental frequency). After calculating the positive sequence current signal, the resulting current signals are implemented using the DWT to decompose the high-frequency components, and the obtained signals are plotted in the bottom traces of Fig. 6(c) and Fig. 6(d), respectively. This is the same behaviour as in the case of the positive sequence current. Further analysis of Fig. 6(c) reveals that the arrival time is related to the transient wave of the travelling wave, as shown in Fig. 1. The first arrival time and same wave reflected back are clearly indicated; this indicates that the arrival time of a transient wave from the DWT can be beneficial in calculating lightning location. In addition, after the lightning strikes, the coefficient detail of the positive sequence current from the DWT increases immediately, and the first order of the transient wave (t_{1stRYG}) is higher than that of the other transient wave (t_{2ndRYG}) and the same wave reflected back (t_{3rdRYG}). This indicates that the decision algorithm for abnormal detection can benefit from variations of the coefficient detail.

By performing many case studies, the locations of lightning strikes, peak value of lightning, inception angles of lightning strikes, and ground resistances of transmission tower were varied, to understand the transient wave behaviour and

the variation in arrival time. The obtained results indicate that the arrival time of the transient wave from the positive sequence current signal in cases with and without DWT have the same behaviour, as shown in Table 4. Moreover, the arrival time in scale 1 from the DWT seems adequate for detecting the arrival time; therefore, it is unnecessary to use the arrival time from higher scales.

By considering cases with and without DWT, as shown in Table 4, when the location of lightning was varied and the inception angles do not change, the arrival time at the sending substation tends to significantly increase with the increase in distance between the sending substation and the position of lightning, while the arrival time of receiving substation tends to decrease; this is owing to the effects of the impedance of the transmission line.

Based on a further analysis of Table 4, by changing the peak value of the lightning but not its position, it can be observed that the arrival time at both substations has no impact on the increase in the peak value of the lightning; because of this, the characteristics of the transient wave and velocity of the transient wave depend on the impedance of the conductor (inductance and capacitance) on the transmission line. Similarly, when considering the ground resistance of the transmission tower, the arrival time at both substations has little or no impact on the increase in the ground resistance; this behaviour is the same as that in the other case studies. Thus, these parameters were ignored in this study.

In addition, it can be seen that the arrival times obtained with and without the DWT are clearly different, and these two different times will be compared to the lightning location in the next section.

By observing the data in Table 5, when the sensor G and sensor H was installed between stations at $L/3$ km, and $2L/3$ km, respectively, the arrival time of both sensors was recorded as shown in Table 5. The characteristic of a transient wave tends to significantly increase with the increasing of distance between the sending substation and position of lightning; this behaviour is the same as that observed in case studies of Table 4. For the next section, the result of lightning location was achieved.

IV. RESULTS AND DISCUSSION

The characteristics of a transient wave when lightning occurs in the system were explained in previous sections. The arrival times based on the three proposed techniques were recorded in Table 4 and Table 5 to calculate the lightning location, and the obtained results and average error are shown in Table 6. Moreover, to ascertain the advantages of the proposed technique, the lightning location with the type D travelling wave method (without DWT) was compared with all proposed techniques, and the obtained results are shown in Table 6. From Table 6, the average error using the type D travelling wave method (without DWT) is 0.8079 km, that is, a higher error than all other techniques. Therefore, the proposed technique with DWT is superior to the conventional technique, and can improve the accuracy of calculation.

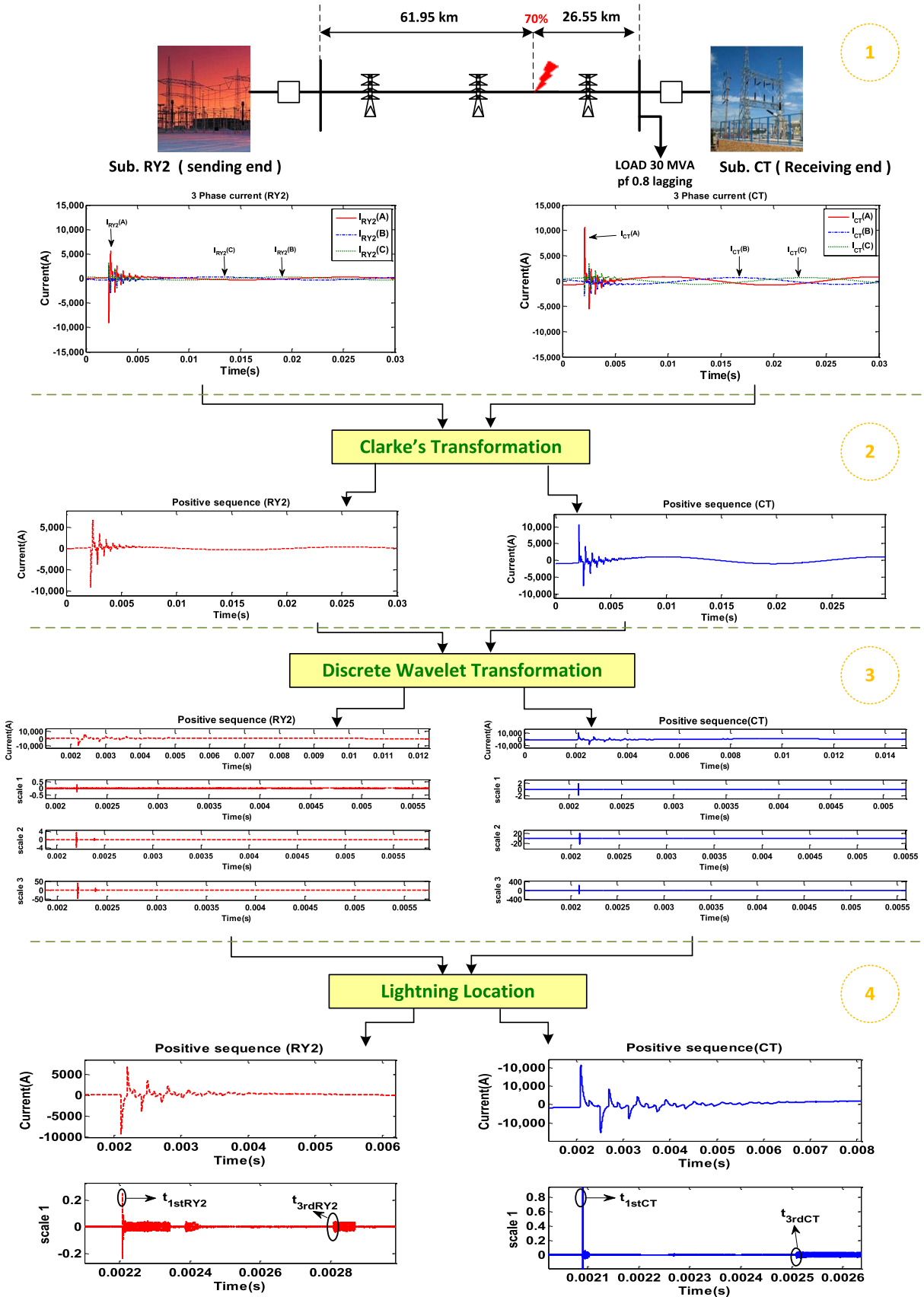


FIGURE 5. Operation in this experimentation.

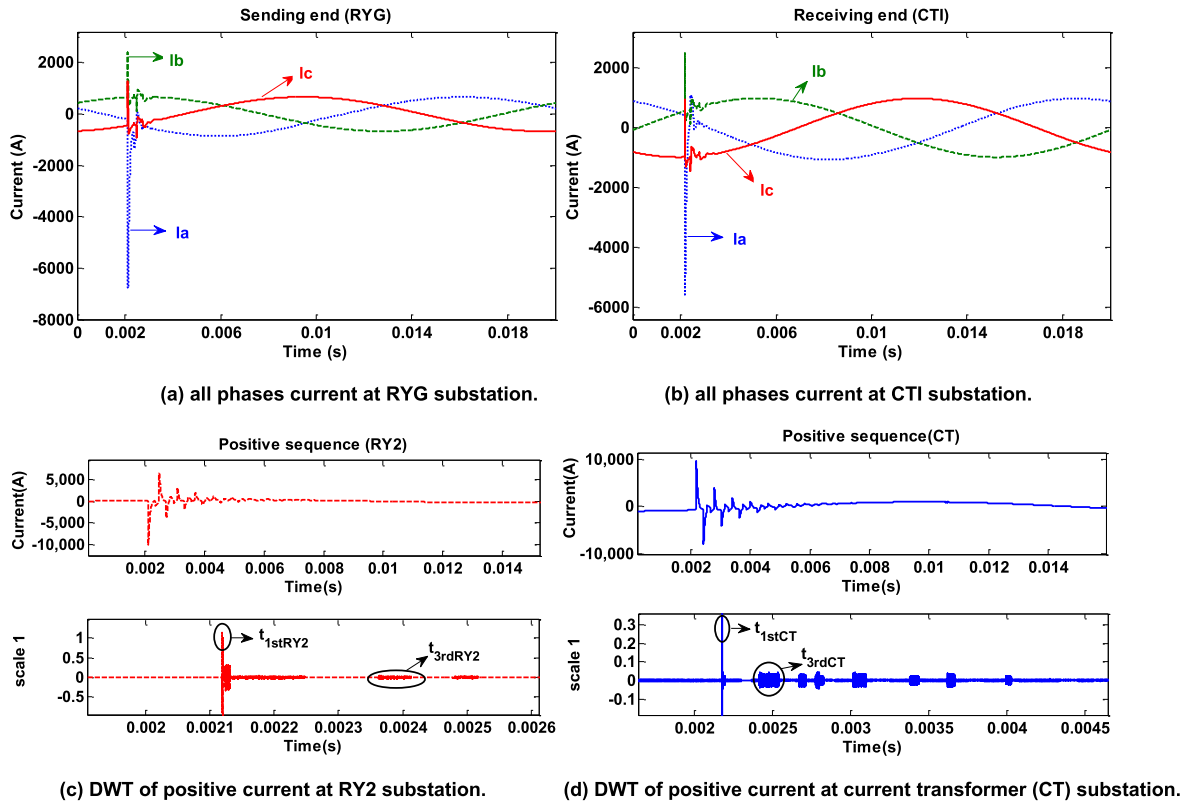


FIGURE 6. Lightning strike at 40% of transmission line length.

TABLE 4. Arrival time at both the ends of substation in cases without discrete wavelet transform (DWT) and with DWT.

Parameters	Positive sequence without DWT		Positive sequence with DWT			
	Sending Substation	Receiving substation	Sending Substation		Receiving substation	
	t_{1stRYG}	t_{1stCTI}	t_{1stRYG}	t_{3rdRYG}	t_{1stCTI}	t_{3rdCTI}
% Length of transmission line						
10%	0.0020332	0.0022806	0.002030	0.002088	0.002266	0.002799
20%	0.0020648	0.0022500	0.002059	0.002177	0.002237	0.002710
30%	0.0020962	0.0022195	0.002089	0.002265	0.002207	0.002621
40%	0.0021273	0.0021887	0.002118	0.002355	0.002178	0.002533
50%	0.0021580	0.0021580	0.002148	0.002443	0.002148	0.002444
60%	0.0021886	0.0021271	0.002178	0.002533	0.002118	0.002355
70%	0.0022193	0.0020960	0.002207	0.002621	0.002089	0.002265
80%	0.0022498	0.0020648	0.002237	0.002710	0.002059	0.002177
90%	0.0022796	0.0020332	0.002266	0.002798	0.002030	0.002088
Current of lightning strikes						
10 kA	0.0021273	0.0021887	0.002118	0.002355	0.002178	0.002533
20 kA	0.0021273	0.0021887	0.002118	0.002355	0.002178	0.002533
30 kA	0.0021273	0.0021887	0.002118	0.002355	0.002178	0.002533
Ground resistance of transmission tower						
1	0.0021273	0.0021887	0.002118	0.002354	0.002178	0.002533
10	0.0021273	0.0021887	0.002118	0.002355	0.002178	0.002533
100	0.0021273	0.0021887	0.002118	0.002354	0.002177	0.002533

TABLE 5. Arrival time at both sensors in case with DWT.

% Length of transmission line	Sending station (RY2)		Receiving station (CTI)	
	t_{G1}	t_{G2}	t_{H1}	t_{H2}
10%	0.002071	0.002131	0.002171	0.0022343
20%	0.002040	0.002159	0.002140	0.002259
30%	0.002010	0.0021901	0.002110	0.0022902
40%	0.002020	0.002219	0.002080	0.0022787
50%	0.002050	0.002250	0.002050	0.0022525
60%	0.002080	0.002279	0.002020	0.0022189
70%	0.002111	0.002295	0.002010	0.0021901
80%	0.002140	0.002259	0.002040	0.0021594
90%	0.002169	0.002229	0.002070	0.0021295

In Table 4, the first arrival times for each substation were used to calculate the lightning location, based on a combination of the type D travelling wave method and the DWT, with the velocity of the travelling wave set as 298,782 km/s (as shown in Table 1 and Fig. 2). By considering the obtained result in Table 6, it can be seen that the average error is 0.08237 km.

For lightning location based on a combination of the type A and D travelling wave methods and the DWT, the first arrival time and that of the same wave reflected back for each substation were used for calculating the lightning location with Equation 2 without using the velocity of the travelling wave, as shown in Table 4. The results are also shown in Table 6, where the average error is 0.08992 km.

In Table 5, and according to the single-line diagram shown in Fig. 3, the arrival times of the transient wave recorded with sensor G and sensor H (at $L/3$ km, $2L/3$ km) were used to calculate the lightning location with Equations 5–10. The average error is 0.06798 km, as shown in Table 6.

As a result, by considering the average error in Table 6, it can be shown that lightning location using method 1 (based on combination of travelling wave type D and the DWT) is more efficient as compared to using other techniques.

Further, to evaluate and show the advantages of the proposed technique, the proposed techniques were used not only for identifying the location of a lightning strike, but also for locating faults in the transmission system, as shown in Table 7. As seen in Table 7, the location of the single-line-to-ground faults were varied, and the three proposed techniques were compared. The obtained result shows that all of the proposed techniques provide satisfactory results. In particular, the average error of the technique using two sensors is less than 0.03395 km, when compared with other techniques.

According to the results in Table 6 and Table 7, it can be clearly seen that the overall results of the proposed technique are satisfactory, with an average error of less than

0.1 km, which is significantly less than the conventional technique (the lightning location with the type D travelling wave method without the DWT). This indicates that the proposed technique is useful for identifying the location of abnormal conditions in the transmission system. Moreover, the obtained average error from the arrival time of the transient wave recorded with two sensors gives better results than the other techniques, in cases of both lightning location and fault location. When the lightning location is based on the combination of the type D travelling wave method and the DWT, the accuracy of this technique depends on the velocity of the transient wave and the first arrival time at both substations; this is the highlight, as the first arrival time at each substation is easy to observe or detect. Accordingly, the result from this technique is highly satisfactory. However, this technique can only be used for transmission systems with two buses and, when applied to a complex transmission system (more than two buses), it may cause difficulties in calculating the lightning location.

When the lightning location is based on a combination of the type A and D travelling wave methods and the DWT, the accuracy is satisfactory as compared to a conventional technique, but is less than that of the other technique. This technique uses many arrival times (first and same wave reflecting back at both substations); this is a disadvantage, as while the first arrival time can be easily observed, the other arrival time is difficult to detect and/or may be inaccurately detected.

Although the lightning location method based on two sensors uses many arrival times, this technique imitates the travelling wave equations. This is to say, during lightning strikes within zone 1 or zone 3, Equation 6 will have a calculation model identical to the type A travelling wave method equation, whereas during the lightning strikes within zone 2, Equation 8 will have a calculation model identical to the type D travelling wave method. In addition, the velocity of the transient wave in each zone will

TABLE 6. Results of the lightning location.

% Length of transmission line	Actual position (km)	Travelling wave without DWT		Travelling wave type A and D with DWT		Travelling wave type D with DWT			Two sensors with DWT		
		Calculation (km)	Error (km)	Calculation (km)	Error (km)	Velocity (km/s)	Calculation (km)	Error (km)	Velocity (km/s)	Calculation (km)	Error (km)
10%	8.85000	7.29067	1.55933	8.68528	0.16472	298,782	8.99372	0.14372	295,000	8.85000	0.00000
20%	17.70000	16.58279	1.11721	17.67005	0.02995	298,782	17.65840	0.04160	295,000	17.55250	0.14750
30%	26.55000	25.83009	0.71991	26.40000	0.15000	298,782	26.62186	0.07186	295,000	26.56475	0.01475
40%	35.40000	35.07739	0.32261	35.42990	0.02990	298,782	35.28654	0.11346	296,706	35.34881	0.05119
50%	44.25000	44.25000	0.00000	44.17513	0.07487	298,782	44.25000	0.00000	293,179	44.25000	0.00000
60%	53.10000	53.43755	0.33755	53.07010	0.02990	298,782	53.21346	0.11346	296,557	53.14671	0.04671
70%	61.95000	62.66991	0.71991	62.10000	0.15000	298,782	61.87814	0.07186	292,079	62.19827	0.24827
80%	70.80000	71.88734	1.08734	70.82995	0.02995	298,782	70.84160	0.04160	295,000	70.88850	0.08850
90%	79.65000	81.05994	1.40994	79.80000	0.15000	298,782	79.50628	0.14372	297,980	79.63510	0.01490
Average error (km)		0.80820		0.08992		0.08237			0.06798		

TABLE 7. Results of the fault location in case of single-line-to-ground fault.

% Length of transmission line	Actual position (km)	Travelling wave type A and D with DWT [54]		Travelling wave type D with DWT [53]			Two sensors with DWT		
		Calculation (km)	Error (km)	Velocity (km/s)	Calculation (km)	Error (km)	Velocity (km/s)	Calculation (km)	Error (km)
10%	8.85000	8.76008	0.08992	298,782	8.93397	0.08397	295,000	8.85000	0.00000
20%	17.70000	17.57558	0.12442	298,782	17.64346	0.05654	295,000	17.55250	0.14750
30%	26.55000	26.43166	0.11834	298,782	26.60692	0.05692	295,000	26.56475	0.01475
40%	35.40000	35.35068	0.04932	298,782	35.45087	0.05087	294,577	35.41269	0.01269
50%	44.25000	44.25000	0.00000	298,782	44.25000	0.00000	293,179	44.25000	0.00000
60%	53.10000	53.14932	0.04932	298,782	53.04913	0.05087	294,584	53.08753	0.01247
70%	61.95000	62.06834	0.11834	298,782	61.89308	0.05692	295,000	61.93525	0.01475
80%	70.80000	70.92442	0.12442	298,782	70.85654	0.05654	295,000	70.88850	0.08850
90%	79.65000	79.60434	0.04566	298,782	79.56603	0.08397	297,980	79.63510	0.01490
Average error (km)		0.07997		0.05518			0.03395		

change according to the arrival time at each zone. Thus, this technique is efficient in predicting the lightning location in both a transmission system with two buses and a complex transmission system, as it uses the arrival time(s) from the sensor.

V. CONCLUSION

This paper proposed three techniques based on the DWT to identify the location of a lightning strike in a 115 kV transmission system over 88.5 km. Case studies of lightning location were simulated using ATP/EMTP program, in which the inception angle, lightning location, and lightning phase were varied. A positive sequence was calculated, then the DWT was applied to decompose the high-frequency components of the signal. After applying the DWT, the arrival time from

the DWT of each substation was investigated based on the travelling wave and DWT, The arrival time from the DWT of two sensors installed at L/3 km and 2L/3 km of the transmission line were also used for calculating the lightning location. In addition, the three proposed techniques are not only suitable for calculating lightning location, but also for calculating fault location. By comparing the three proposed techniques, it can be seen that the technique based on the arrival time of the transient wave which records with two sensors is a powerful tool as it gives satisfactory results for lightning location, as shown in Tables 6–7. Future research will be aimed at increasing the number of sensors and improving the equations, so that the location of lightning along a complex or looped-structure transmission system can be identified.

REFERENCES

- [1] P. Chowdhuri, "Parameters of lightning strokes and their effects on power systems," in *Proc. IEEE/PES Transmiss. Distrib. Conf. Expo. Developing Perspect.*, Nov. 2001, pp. 1047–1051.
- [2] A. Elkalsh, P. Sewell, T. M. Benson, and A. Vukovic, "Coupled electrothermal two-dimensional model for lightning strike prediction and thermal modeling using the TLM method," *IEEE J. Multiscale Multiphys. Comput. Techn.*, vol. 2, pp. 38–48, 2017.
- [3] J.-M. Ge, Y. Shen, W.-B. Yu, R.-T. Liu, W. Fan, and Y.-X. Yang, "A lightning current measurement method based on optical sensing technology," *IEEE Sensors J.*, vol. 19, no. 11, pp. 4250–4258, Jun. 2019.
- [4] S. I. Abouzeid, G. Shabib, and A. Z. El Dein Mohamed, "Induced voltages on overhead transmission lines because of nearby included lightning channel," *IET Gener., Transmiss. Distrib.*, vol. 9, no. 13, pp. 1672–1680, Oct. 2015.
- [5] F. Goll and R. Witzmann, "Lightning protection of 500-kV DC gas-insulated lines (GIL) with integrated surge arresters," *IEEE Trans. Power Del.*, vol. 30, no. 3, pp. 1602–1610, Jun. 2015.
- [6] J. He, X. Wang, Z. Yu, and R. Zeng, "Statistical analysis on lightning performance of transmission lines in several regions of China," *IEEE Trans. Power Del.*, vol. 30, no. 3, pp. 1543–1551, Jun. 2015.
- [7] Y. Long, C. Yao, Y. Mi, J. Wang, X. Tang, and R. Liao, "Preliminary full-waveform inversion of lightning current using differential-integral loop measurement," *IEEE Trans. Dielectr. Electr. Insul.*, vol. 23, no. 3, pp. 1534–1545, Jun. 2016.
- [8] A. Rahiminejad and B. Vahidi, "LPM-based shielding performance analysis of high-voltage substations against direct lightning strokes," *IEEE Trans. Power Del.*, vol. 32, no. 5, pp. 2218–2227, Oct. 2017.
- [9] Y. Li, W. Sima, Q. Yang, J. Li, and T. Yuam, "Optimization of transmission-line route based on lightning incidence reported by the lightning location system," *IEEE Trans. Power Del.*, vol. 28, no. 3, pp. 1460–1468, Jul. 2013.
- [10] G. Yang, Z. Yu, Y. Zhang, S. Chen, B. Zhang, and J. He, "Evaluation of lightning current and return stroke velocity using measured far electric field above a horizontally stratified ground," *IEEE Trans. Electromagn. Compat.*, vol. 59, no. 6, pp. 1940–1948, Dec. 2017.
- [11] S. Visacro, M. Guimaraes, P. Mattioli, and M. H. M. Vale, "Features of upward lightning measured in a tropical region and their potential to cause hazardous effects," *IEEE Trans. Electromagn. Compat.*, vol. 61, no. 3, pp. 745–750, Jun. 2019.
- [12] M. Li, K. Song, Y. Ou, T. Gan, Y. Fan, and J. Chen, "Research on line patrol strategy of 110 kV transmission line after lightning strike," in *Proc. MATEC Web Conf.*, vol. 55, 2016, p. 05004.
- [13] Z. He, "Application of wavelet analysis in high-voltage transmission line fault location," in *Wavelet Analysis and Transient Signal Processing Applications for Power Systems*. Singapore: Wiley, 2016, pp. 130–155, ch. 8.
- [14] H. Jia, "An improved traveling-wave-based fault location method with compensating the dispersion effect of traveling wave in wavelet domain," *Math. Problems Eng.*, vol. 2017, Feb. 2017, Art. no. 1019591.
- [15] E. Volpov and R. Linder, "Application of local environmental data to the lightning performance assessment of the IECO transmission-line network," *IEEE Trans. Power Del.*, vol. 32, no. 6, pp. 2546–2554, Dec. 2017.
- [16] E. Volpov and E. Katz, "Characterization of local environmental data and lightning-caused outages in the IECO transmission-line network," *IEEE Trans. Power Del.*, vol. 31, no. 2, pp. 640–647, Apr. 2016.
- [17] S. Kobayashi, Y. Tanaka, Y. Baba, T. Tsuboi, and S. Okabe, "Computation of lightning electromagnetic pulses using a hybrid constrained interpolation profile and transmission line modeling method," *IEEE Trans. Electromagn. Compat.*, vol. 59, no. 6, pp. 1958–1966, Dec. 2017.
- [18] M. R. Alemi and K. Sheshyekani, "Wide-band modeling of tower-footing grounding systems for the evaluation of lightning performance of transmission lines," *IEEE Trans. Electromagn. Compat.*, vol. 57, no. 6, pp. 1627–1636, Dec. 2015.
- [19] C. Vilacha, A. F. Otero, J. C. Moreira, and E. Miguez, "Analysis of a grounding system under a lightning stroke," *IEEE Trans. Ind. Appl.*, vol. 51, no. 6, pp. 4907–4911, Mar. 2015.
- [20] H. Lu, Z. Feng, X. Tong, W. Chen, B. Tan, and X. Wen, "Observation and analysis of the sparkover around grounding electrode under impulse current," *IET Gener., Transmiss. Distrib.*, vol. 11, no. 8, pp. 1997–2002, Jun. 2017.
- [21] Y. Huangfu, S. Wang, and X. Tao, "Transient lightning impulse performance analysis for composite transmission line tower," *IEEE Trans. Electromagn. Compat.*, vol. 57, no. 5, pp. 1103–1111, Oct. 2015.
- [22] Y. He, Z. Fu, B. Wei, J. Chen, and A. Jiang, "Dynamic characteristics and cascaded coordination of limiting-type SPDs under subsequent negative strokes," *IET Gener., Transmiss. Distrib.*, vol. 10, no. 16, pp. 4197–4204, Dec. 2016.
- [23] R. Ismail and Z. A. Baharudin, "A review on basic principle of lightning location in multi-station system and the ability of single-station measurement," in *Proc. IEEE Int. Conf. Power Energy (PECon)*, Nov. 2016, pp. 62–67, doi: 10.1109/PECON.2016.7951534.
- [24] F. Diaz, C. Gomez, and F. Roman, "Time delay measurement based on analytic signal for lightning interferometer," in *Proc. 35th Int. Conf. Lightning Protection (ICLP) 16th Int. Symp. Lightning Protection (SIPDA)*, Sep. 2021, pp. 1–4, doi: 10.1109/ICLPandSIPDA54065.2021.9627481.
- [25] R. E. Jimenez and J. G. Herrera, "Location of direct lightning impacts to overhead transmission lines by means of a time of arrival algorithm," in *Proc. North Amer. Power Symp. (NAPS)*, Sep. 2012, pp. 1–6, doi: 10.1109/NAPS.2012.6336356.
- [26] R. Razzaghi, M. Scatena, K. Sheshyekani, M. Paolone, F. Rachidi, and G. Antonini, "Locating lightning strikes and flashovers along overhead power transmission lines using electromagnetic time reversal," *Electr. Power Syst. Res.*, vol. 160, pp. 282–291, Jul. 2018.
- [27] S. Das, S. Santoso, A. Gaikwad, and M. Patel, "Impedance-based fault location in transmission networks: Theory and application," *IEEE Access*, vol. 2, pp. 537–557, 2014.
- [28] A. H. Al-Mohammed and M. A. Abido, "A fully adaptive PMU-based fault location algorithm for series-compensated lines," *IEEE Trans. Power Syst.*, vol. 29, no. 5, pp. 2129–2137, Sep. 2014.
- [29] C. Paul, F. H. Heidler, and W. Schulz, "Performance of the European lightning detection network EUCLID in case of various types of current pulses from upward lightning measured at the Peissenberg tower," *IEEE Trans. Electromagn. Compat.*, vol. 62, no. 1, pp. 116–123, Feb. 2020.
- [30] H. G. P. Hunt, K. J. Nixon, I. R. Jandrell, and W. Schulz, "Can we model the statistical distribution of lightning location system errors better?" *Electr. Power Syst. Res.*, vol. 178, Jan. 2020, Art. no. 106042.
- [31] Y. Long, C. Yao, Y. Mi, D. Hu, N. Yang, and Y. Liao, "Identification of direct lightning strike faults based on Mahalanobis distance and S-transform," *IEEE Trans. Dielectr. Electr. Insul.*, vol. 22, no. 4, pp. 2019–2030, Aug. 2015.
- [32] M. Davoudi, J. Sadeh, and E. Kamyab, "Transient-based fault location on three-terminal and tapped transmission lines not requiring line parameters," *IEEE Trans. Power Del.*, vol. 33, no. 1, pp. 179–188, Feb. 2018.
- [33] G. Karnas, G. Maslowski, and P. Baranski, "A novel algorithm for determining lightning leader time onset from electric field records and its application for lightning channel height calculations," *Electr. Power Syst. Res.*, vol. 178, Jan. 2020, Art. no. 106021.
- [34] Y. Xi, Y. Cui, X. Tang, Z. Li, and X. Zeng, "Fault location of lightning strikes using residual analysis based on an adaptive Kalman filter," *IEEE Access*, vol. 7, pp. 88126–88137, 2019.
- [35] J. A. Morales, Z. Anane, and R. J. Cabral, "Automatic lightning stroke location on transmission lines using data mining and synchronized initial travelling," *Electr. Power Syst. Res.*, vol. 163, pp. 547–558, Oct. 2018.
- [36] X. Dong, J. Wang, S. Shi, B. Wang, B. Dominik, and M. Redefern, "Traveling wave based single-phase-to-ground protection method for power distribution system," *CSEE J. Power Energy Syst.*, vol. 1, no. 2, pp. 75–82, Jun. 2015.
- [37] L. Tang, X. Dong, S. Luo, S. Shi, and B. Wang, "A new differential protection of transmission line based on equivalent travelling wave," *IEEE Trans. Power Del.*, vol. 32, no. 3, pp. 1359–1369, Jun. 2017.
- [38] R. J. Hamidi and H. Livani, "Traveling-wave-based fault-location algorithm for hybrid multiterminal circuits," *IEEE Trans. Power Del.*, vol. 32, no. 1, pp. 135–144, Feb. 2017.
- [39] R. J. Hamidi, H. Livani, and R. Rezaiesarlak, "Traveling-wave detection technique using short-time matrix pencil method," *IEEE Trans. Power Del.*, vol. 32, no. 6, pp. 2565–2574, Mar. 2017.
- [40] C. M. de Sousa Neto, F. B. Costa, R. L. de Araujo Ribeiro, R. L. Barreto, and T. de Oliveira Alves Rocha, "Wavelet-based power system stabilizer," *IEEE Trans. Ind. Electron.*, vol. 62, no. 12, pp. 7360–7369, Dec. 2015.
- [41] J. A. Antonino-Daviu, J. Pons-Llinares, and S. B. Lee, "Advanced rotor fault diagnosis for medium-voltage induction motors via continuous transforms," *IEEE Trans. Ind. Appl.*, vol. 52, no. 5, pp. 4503–4509, Sep. 2016.
- [42] R. P. Medeiros, F. B. Costa, and K. M. Silva, "Power transformer differential protection using the boundary discrete wavelet transform," *IEEE Trans. Power Del.*, vol. 31, no. 5, pp. 2083–2095, Oct. 2015.

- [43] D. Guillen, M. R. A. Paternina, A. Zamora, J. M. Ramirez, and G. Idarraga, "Detection and classification of faults in transmission lines using the maximum wavelet singular value and Euclidean norm," *IET Gener., Transmiss. Distrib.*, vol. 9, no. 15, pp. 2294–2302, Nov. 2015.
- [44] K. A. Saleh, A. Hooshyar, and E. F. El-Saadany, "Hybrid passive-overcurrent relay for detection of faults in low-voltage DC grids," *IEEE Trans. Smart Grid*, vol. 8, no. 3, pp. 1129–1138, May 2017.
- [45] F. B. Costa, B. A. Souza, N. S. D. Brito, J. A. C. B. Silva, and W. C. Santos, "Real-time detection of transients induced by high-impedance faults based on the boundary wavelet transform," *IEEE Trans. Ind. Appl.*, vol. 51, no. 6, pp. 5312–5323, Nov. 2015.
- [46] A. R. Adly, R. A. E. Sehiemy, A. Y. Abdelaziz, and N. M. A. Ayad, "Critical aspects on wavelet transforms based fault identification procedures in HV transmission line," *IET Gener., Transmiss. Distrib.*, vol. 10, no. 2, pp. 508–517, Feb. 2016.
- [47] U. Sonnadara, V. Kathirarachchi, V. Cooray, R. Montano, and T. Götschl, "Performance of lightning locating systems in extracting lightning flash characteristics," *J. Atmos. Solar-Terrestrial Phys.*, vol. 112, pp. 31–37, May 2014.
- [48] Z. Yi and A. H. Etemadi, "Line-to-line fault detection for photovoltaic arrays based on multiresolution signal decomposition and two-stage support vector machine," *IEEE Trans. Ind. Electron.*, vol. 64, no. 11, pp. 8546–8556, May 2017.
- [49] A. A. P. Biscaro, R. A. F. Pereira, M. Kezunovic, and J. R. S. Mantovani, "Integrated fault location and power-quality analysis in electric power distribution systems," *IEEE Trans. Power Del.*, vol. 31, no. 2, pp. 428–436, Aug. 2015.
- [50] A. Swetapadma and A. Yadav, "A novel decision tree regression-based fault distance estimation scheme for transmission lines," *IEEE Trans. Power Del.*, vol. 32, no. 1, pp. 234–245, Aug. 2016.
- [51] K. Park, Y. Motai, and J. R. Yoon, "Acoustic fault detection technique for high-power insulators," *IEEE Trans. Ind. Electron.*, vol. 64, no. 12, pp. 9699–9708, Jun. 2017.
- [52] C. Apisit and A. Ngaopitakkul, "Algorithm improvement to predict fault location of simultaneous fault in underground cable," *IEEE Trans. Power Energy*, vol. 133, no. 11, pp. 799–805, 2013.
- [53] P. Chiradeja and C. Pothisarn, "Identification of the fault location for three-terminal transmission lines using discrete wavelet transforms," in *Proc. Transmiss. Distrib. Conf. Expo., Asia Pacific*, Seoul, South Korea, Oct. 2009, pp. 1–4.
- [54] C. Pothisarn, C. Jettanasen, A. Ngaopitakkul, and C. Apisit, "Identification of fault location for simultaneous fault in distribution system using discrete wavelet transform," *ICIC Exp. Lett.*, vol. 5, no. 4, pp. 1423–1428, 2011.
- [55] A. Ngaopitakkul and S. Bunjongjit, "An application of a discrete wavelet transform and a back-propagation neural network algorithm for fault diagnosis on single-circuit transmission line," *Int. J. Syst. Sci.*, vol. 44, no. 9, pp. 1745–1761, Sep. 2013.



PATHOMTHATH CHIRADEJA received the B.Eng. degree from Kasetsart University, Bangkok, Thailand, the M.S. and Ph.D. degrees from Oklahoma State University (OSU), Stillwater, OK, USA, all in electrical engineering. He is an Assistance Professor with the Department of Electrical Engineering, Faculty of Engineering, Srinakharinwirot University, Thailand. His research interests include power systems, renewable energy systems, power economics, and distributed generation systems.



ATHTHAPOL NGAOPITAKKUL received the B.Eng., M.Eng., and D.Eng. degrees in electrical engineering from the King Mongkut's Institute of Technology Ladkrabang, Bangkok, Thailand, in 2002, 2004, and 2007, respectively. He is currently an Associate Professor with the Department of Electrical Engineering, Faculty of Engineering, King Mongkut's Institute of Technology Ladkrabang. His research interests include application of wavelet transform, AI for transmission systems, and protection relay.

...